PRAMANA
— journal of
physics

© Printed in India

Vol. 44, No. 6,
June 1995
pp. 545–553

Elastic scattering of 81 keV γ rays by aluminium, nickel, tantalum, gold and lead

G BASAVARAJU[1], P P KANE[1], LYNN KISSEL[2,*] and R H PRATT[2]
[1] Department of Physics, Indian Institute of Technology, Powai, Bombay 400 076, India
[2] Department of Physics and Astronomy, University of Pittsburgh, Pittsburgh, PA 15260, USA
*Permanent address: Computational Physics Group, Lawrence Livermore National Laboratory, Livermore, CA 94550, USA

MS received 5 December 1994; revised 18 March 1995

Abstract. A recently reported study [*Phys. Rev.* **A49**, 3664 (1994)] of elastic scattering of 81 keV γ rays in the angular range from 60° to 133° has been extended to smaller and larger angles. Previously reported S matrix calculations of atomic Rayleigh scattering have been shown to require a subtraction of contributions from spurious resonances. Most of the experimental data are in agreement with the calculations. Calculations (MF + ASF) based on a combination of relativistic modified form factors (MF's) and angle independent anomalous scattering factors (ASF's) are found to be inadequate for an explanation of experimental cross-sections in the case of high Z elements at angles larger than about 120°.

Keywords. Germanium detector; anomalous scattering; S matrix.

PACS No. 32·80

1. Introduction

Recently, a study of elastic scattering of 81 keV γ rays has been reported [1] in the angular range from 60° to 133°. The experimental results were found to be in reasonable agreement with the then reported relativistic second order S matrix calculations of atomic Rayleigh scattering, but, at large angles in the case of high Z elements, were in poorer agreement with (MF + ASF) calculations based on a combination of relativistic modified factors (MF's) and angle independent anomalous scattering factors (ASF's). As expected for photon energies close to or less than target K shell binding energies, ε_K, a simple treatment based on only MF's was shown to fail in the case of gold and lead with ε_K values of 80·723 and 88·006 keV, respectively.

The experimental cross-sections at 133° in the case of tantalum and gold, and at 120° and 133° in the case of lead were found to be significantly smaller than (MF + ASF) calculations. The present studies at 145° confirm the same trend at a larger angle. The cross-sections for the elastic scattering of 81 keV γ rays increase rapidly below about 90° with decreasing angle θ, whereas the cross-sections for the production of $K\beta'_2$ X-rays are independent of angle. Thus, in the case of gold with $K\beta'_2$ X-rays having energies from about 80·08 to 80·72 keV, the determination of the 81 keV elastic scattering counts from a composite pulse height distribution in the 80 to 81 keV range was expected to become easier at smaller angles of scattering. On the other hand, on account of decreasing Compton shifts, a separation of the elastic and the broad Compton peaks becomes increasingly more difficult as θ decreases. An angle of 45° was found to be optimal from these considerations.

Previously reported S matrix calculations were shown to require a subtraction of contributions from "spurious" resonances, which are particularly significant when the photon energy is close to an inner shell threshold. These features and the new calculations are described in § 2. Important details relevant to the new measurements are mentioned in § 3. The experimental and theoretical results at six angles from 45° to 145°, including some of the earlier ones, are presented in § 4.

2. Theoretical calculations

The elastic scattering cross-sections have been calculated for isolated atoms, since solid state environment effects are not expected to be significant for values of the momentum transfer parameter $x[=\sin(\theta/2)/\lambda(\text{Å})]$ larger than about 2·5 relevant for the present study. The relativistic calculations have been performed in the independent particle approximation for bound electrons. The scattering amplitude for each atomic electron is evaluated separately and is summed so as to obtain the atomic Rayleigh amplitude. In the second order S matrix treatment, the contribution of each electron involves a sum over a complete set of intermediate states (bound and continuum) of the single particle Hamiltonian. As pointed out in [2], transitions to intermediate bound states correspond to resonances in the individual electron amplitude. The resonant contribution from an electron in a bound state (a) involving an intermediate occupied state (b) is cancelled by the resonance in the amplitude for scattering from an electron in state (b) involving the intermediate state (a). These cancelling resonances are called "spurious" resonances. The scattering amplitude of an electron is small below the resonance regime and is proportional to the square of the photon energy in the low energy limit. When the photon energy is larger than the photoionization threshold associated with a given electron, the scattering amplitude for that electron is close to r_0 in the forward direction but generally becomes small for scattering vectors [= (momentum transfers)/$\hbar$] large compared to the inverse of the radius of the orbital. Here, r_0 is e^2/mc^2, e is the electron charge, m is the mass of an electron, c is the speed of light and $h[=2\pi\hbar]$ is Planck's constant. Note that the amplitude is not small in the vicinity of a real or a spurious resonance.

The scattering amplitude at a given finite angle due to weakly bound outer electrons generally drops rapidly with increasing photon energy, hν. Thus approximate estimates of outer electron contributions are adequate and are frequently obtained in the relativistic modified form factor (MF) approximation, whereas it is necessary to treat inner electron shells by S matrix methods. Such a procedure was adopted in many earlier calculations [e.g. 1, 2].

However, the (MF) approximation omits spurious resonances and hence does not provide the proper cancellation with the spurious resonances of the S matrix calculation for the inner shells. The resulting errors become particularly significant when the photon energy is close to an inner shell threshold. Under these circumstances, it is better to first subtract the spurious resonances in the inner shell contributions and to ensure that the amplitude for each shell is finite except for real observable resonances at transitions into unfilled shells. The bound-bound resonant term in each amplitude is calculated with the help of the formulae given in § 2.1 of ref. [2]. Further, as described in ref. [1], it is necessary to adopt a photon energy shifting procedure near an inner shell threshold in order to correctly position the anomalous scattering regime with a rapidly varying amplitude. As in ref. [1], the inner subshells with binding energies larger than hν/300 were treated by S matrix methods and the (MF) approximation was used for the outer shells.

Table 1. Cross-sections for elastic scattering of 81 keV γ rays in 10^{-24}cm^2/sr. The theoretical values are obtained by the coherent addition of nuclear Thomson and atomic Rayleigh contributions. The values (MF + ASF) in column 2 have been obtained on the basis of a combination of relativistic modified form factors (MF) and angle independent anomalous scattering factors (ASF). The cross-sections calculated by the relativistic second order S matrix treatment after subtraction of contributions of spurious resonances are given in column 3. The term SR indicates these contributions. The experimental cross-sections σ_{expt} along with errors $\pm \Delta$ appear in column 4. Note that the experimental values marked with a * for angles between 60° and 133° are the same as those in ref. [1]. If σ_s is the calculated S matrix cross-section in column 3 and $\chi_s = (\sigma_{expt} - \sigma_s)/\Delta$, χ_s^2 is listed in the last column. The average values of χ_s^2 for Al, Ni, Ta, Au and Pb are 0·46, 2·9, 0·09, 0·52 and 1·2, respectively. The average values of similarly defined $(\chi_{MF+ASF})^2$ are 0·46, 4·2, 1·5, 1·7 and 6·5, respectively.

θ (deg)	Calculated cross section (b/sr) (MF + ASF)	Calculated cross section (b/sr) S matrix (after SR, subtraction)	σ_{expt}(b/sr)	χ_s^2
Al				
45	0·0577	0·0573	0·0550 ± 0·0038	0·37
60	0·0241	0·0238	0·0222 ± 0·0026*	0·38
90	0·00510	0·00504	0·00582 ± 0·00070*	1·2
120	0·00237	0·00235	0·00263 ± 0·00033*	0·72
133	0·00206	0·00203	0·00196 ± 0·00030*	0·05
145	0·00190	0·00186	0·00183 ± 0·00033	0·01
Ni				
45	0·409	0·401	0·480 ± 0·034	5·4
60	0·147	0·141	0·125 ± 0·011*	2·1
90	0·0571	0·0544	0·0570 ± 0·0043*	0·37
120	0·0501	0·0477	0·0505 ± 0·0040*	0·49
133	0·0524	0·0495	0·0397 ± 0·0042*	5·4
145	0·0549	0·0514	0·0430 ± 0·0043	3·8
Ta				
45	6·31	6·12	6·05 ± 0·42	0·03
60	2·49	2·35	2·35 ± 0·20*	0·00
90	0·907	0·839	0·843 ± 0·096*	0·00
120	0·836	0·761	0·741 ± 0·082*	0·06
133	0·893	0·799	0·783 ± 0·083*	0·04
145	0·953	0·838	0·788 ± 0·079	0·40
Au				
45	4·15	4·03	4·18 ± 0·46	0·11
60	1·43	1·35	1·26 ± 0·19*	0·22
90	0·445	0·393	0·386 ± 0·058*	0·01
120	0·496	0·423	0·549 ± 0·082*	2·4
133	0·579	0·481	0·461 ± 0·069*	0·08
145	0·663	0·537	0·495 ± 0·074	0·32
Pb				
45	6·74	6·43	6·30 ± 0·44	0·09
60	2·71	2·50	2·21 ± 0·17*	2·9
90	0·588	0·523	0·518 ± 0·045*	0·01
120	0·399	0·349	0·314 ± 0·033*	1·1
133	0·400	0·344	0·304 ± 0·030*	1·8
145	0·409	0·346	0·310 ± 0·031	1·3

But unlike in ref. [1], spurious resonances in inner shell amplitudes were subtracted off. This procedure is efficient in terms of computation time and is also reliable [3].

The differences between cross-sections calculated before and after subtraction of spurious resonances depend on scattering angle and are of the order of 0·1%, 0·2%, 0·6% and 1·5% for Al, Ni, Ta and Pb, respectively. However, the differences are as much as 13% at 60° in the case of gold with the value of ε_K within 275 eV of hν.

The sensitivity of the new calculations to the value of $(h\nu - \varepsilon_K)$ was checked in the case of gold. For $(h\nu - \varepsilon_K)$ of (275 ± 10) eV, the calculated cross-sections differed at most by $\pm 0{\cdot}9\%$. As seen from table 1, the (MF + ASF) results in column 2 are systematically larger than the S matrix values in column 3. The differences between columns 2 and 3 increase with increasing angle of scattering, and at 145° are about 2·2%, 7·0%, 14%, 23% and 18% for Al, Ni, Ta, Au and Pb, respectively.

The (MF) cross-sections have been shown graphically in [1] over an extensive angular range, and are enormously larger than experimental values for gold and lead. For these reasons, these calculations are not listed in table 1.

3. Measurements

A thin ^{133}Ba source of about 20 mCi strength and 0·1 cm diameter provided 81 keV γ rays, a stronger intensity of 356 keV γ rays and weaker intensities of γ rays of 53·2, 79·6, 160·6, 223·1, 276·4 and 383 keV [4]. A cylindrical brass shell of 15·5 cm diameter and 18 cm length contained lead shielding with the source at its centre. The γ rays from the source emerged through a collimator of 0·8 cm diameter and 10 cm length (figure 1). The heavy source assembly was mounted on a robust arm which could be rotated on a graduated base plate B of 45 cm radius about the vertical direction through the target centre. The source assembly could be moved horizontally along guiding rails towards or away from the target and vertically by screw-jacks. The beam line was more than 25 cm above the base plate. The source-target distance was 23 cm and 31 cm for 45° and 145° measurements, respectively. The 2·54 × 2·54 cm targets of better than 99·5% purity were thin enough to ensure with the adopted orientations, a transmission larger than 0·55 for elastically scattered γ rays.

The distance from the target to the centre of the planar high purity germanium (HpGe) detector was fixed at 23 cm. The HpGe detector supplied by EG & G ORTEC had a diameter of 1·6 cm and a thickness of 1·0 cm, and was cooled in a cryostat with a 0·0127 cm thick beryllium entrance window. A cylindrically symmetric brass shell containing tightly packed tungsten carbide powder was used as the shield around the detector. The opening in front of the detector had a diameter of 2 cm. The detector shield was positioned horizontally on a thick brass plate which could be moved vertically by screw-jacks. The different mechanical parts were fabricated in the workshop of the Department of Physics in Indian Institute of Technology, Bombay.

The pulse height spectrum of γ rays of energies near 81 keV scattered by a 0·360 g/cm^2 nickel target is shown in figure 2. Note that the intensity of 79·6 keV γ rays is only about 8·14% of that of 81 keV γ rays [4]. A weak continuum due to higher energy γ rays underlying the 81 keV photopeak was subtracted in order to determine the net 81 keV elastic scattering counts N_{el} which were about 20 per hour at 145° in the case of aluminium and as high as 500 per hour at 45° in the case of nickel, whereas background counts varied from about 20 per hour at 145° to about 45 per hour at 45°. The error in the estimation of the continuum was combined with the statistical error in order to determine the error in N_{el}. The procedures for the determination of elastic

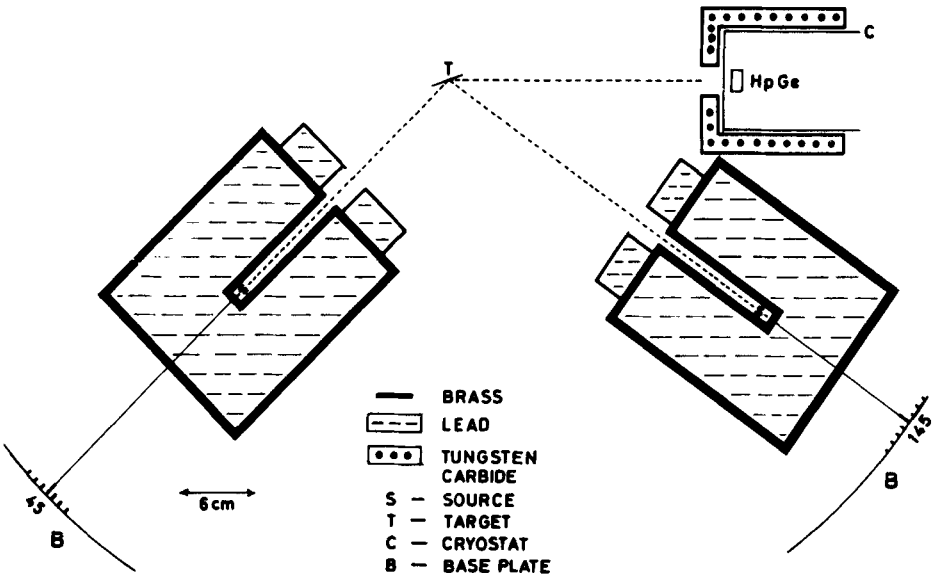

Figure 1. Geometrical arrangement for the scattering experiment (see also § 3). The brass-lead shielding surrounding the source S and the brass-tungsten carbide shielding around the HpGe detector cryostat C are shown. The detector along with its shielding was kept fixed, whereas the distance of the source from the target T was varied from 23 cm for 45° measurements to 31 cm for 145°. The orientation of the target during 45° measurements is shown. But the angle between the incident beam direction and the target plane during 145° measurements was 55° and is not indicated in the interest of clarity of the figure. The source shielding was mounted on a robust arm which could be rotated on the graduated plate B around the vertical direction through the target centre. The height of the beam line above the base plate was larger than 25 cm.

scattering cross-sections have been described in detail [1, 5] but are summarized below in the interest of quick accessibility.

The elastic scattering counts, N_{el}, obtained with a target under study were compared with the Compton scattering counts, N_{Comp}, measured at the same angle with an aluminium target of the same area in order to determine the elastic scattering cross-sections σ_{expt}. This procedure eliminated the need for the determination of the source strength, solid angles, and absolute values of detection efficiency and of target transmissions. The elastic scattering cross-sections were obtained with the help of (1).

$$\frac{N_{el}}{N^{Al}_{Comp}} = \frac{M^t}{M^{Al}} \frac{A^{Al}}{A^t} \frac{T_{81}}{T^{Al}_{Comp}} \frac{\varepsilon_{81}}{\varepsilon_{Comp}} [d\sigma^{Al}_{Comp}/d\Omega]^{-1} \frac{d\sigma_{el}}{d\Omega}, \tag{1}$$

where M^t and M^{Al} are the masses of the target under study and of aluminium, respectively, A^t and A^{Al} are the atomic weights of the target and of aluminium, T_{81} and T^{Al}_{Comp} are the transmissions for 81 keV elastic scattering with the target and for corresponding Compton scattering with aluminium, ε_{81} and ε_{Comp} are the photopeak detection efficiencies for 81 keV and for the energy after Compton scattering, and $d\sigma^{Al}_{Comp}/d\Omega$ is the Compton scattering cross-section of an aluminium atom for 81 keV γ rays. Since the binding energies of electrons in aluminium are much smaller than 81 keV, the last mentioned cross-section is obtained reliably [6] through the use of the

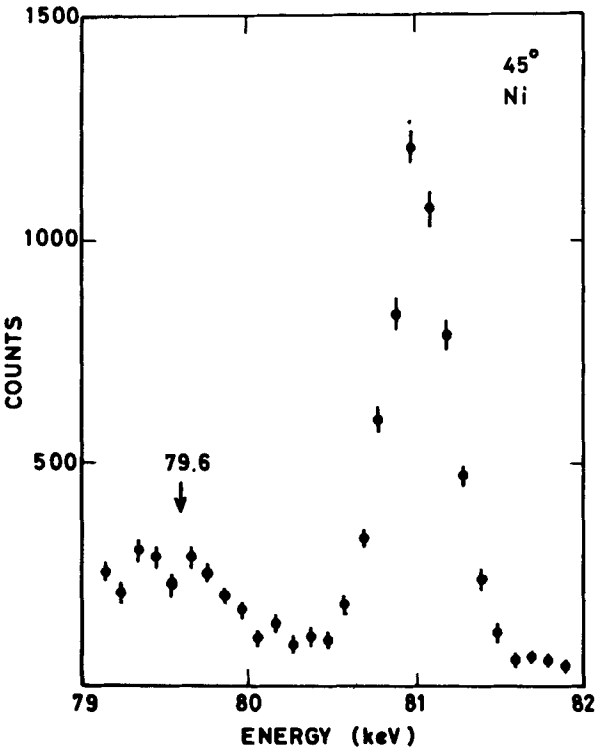

Figure 2. Net counts in the neighbourhood of 81 keV obtained at 45° with a nickel target in 9 h. The small peak corresponding to elastic scattering of the weak 79·6 keV γ ray intensity is indicated by an arrow.

incoherent scattering function $S(x, Z)$, where Z is the atomic number of the scattering atom and x is given by (2).

$$x = \sin(\theta/2)/\lambda(\text{Å}), \tag{2}$$

where θ is the angle of scattering and λ(Å) is the wavelength of the incident radiation in Å. In the case of aluminium, we get

$$\frac{d\sigma^{Al}_{Comp}}{d\Omega} = \frac{d\sigma^{KN}}{d\Omega} S(x, Z = 13), \tag{3}$$

where $d\sigma^{KN}/d\Omega$ is the differential cross-section for Compton scattering by a free and stationary electron according to the well-known Klein–Nishina formula. The shift of the Compton peak from the elastic scattering peak in the pulse height spectrum was used to confirm the scattering angle within about $\pm 0{\cdot}25°$. The Compton peak is broader than the elastic scattering peak on account of finite angular acceptance, $\pm 2°$ in this experiment, and the momentum distribution of electrons in aluminium. The full width at half maximum of the Compton peak was about 1·7 keV. So a correction for the intensity of the weak 79·6 keV Compton component had to be estimated from the relative emission probability of 8·14%, and from the product of values of T^{Al}_{Comp}, ε_{Comp} and $d\sigma^{Al}_{Comp}/d\Omega$ appropriate for 79·6 keV Compton scattering relative to the similarly defined product for 81 keV. The three factors vary slowly with energy and in

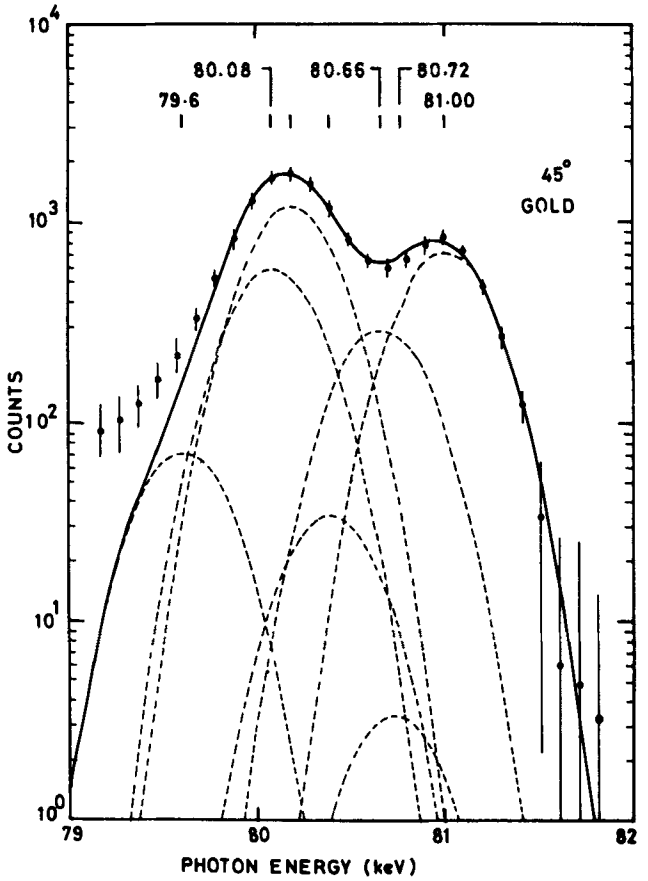

Figure 3. Net counts arising at 45° from gold $K\beta'_2$ X-rays, and elastically scattered 79·6 keV and 81·0 keV γ rays in 40 h. The continuous curve represents the best fit obtained by a least-squares-fitting procedure, the seven dashed curves indicating the corresponding individual contributions as described in § 3. Note the logarithmic scale for counts.

a partially compensating manner. Thus the intensity of the 79·6 keV Compton peak was estimated to be about 8·2% of that in the case of 81 keV Compton scattering and was allowed for in the determination of N^{Al}_{Comp} in (1). The statistical error in N^{Al}_{Comp} was less than 1% but the combined error arising from statistics, and from uncertainties associated with subtraction of the continuum and of the 79·6 keV contribution was conservatively estimated to be $\pm$ 5%.

The transmission factors were calculated with the help of attenuation coefficients interpolated between the values tabulated by Storm and Israel [7]. The error in the ratio of T factors for thin targets in reflection geometry turned out to be about $\pm$ 1·5%. The relative efficiencies of the HpGe detector in the energy range of interest were measured with the help of relative intensities of $K\alpha_2$, $K\alpha_1$, $K\beta'_1$ and $K\beta'_2$ X-rays obtained separately with tantalum, gold and lead targets. As in [1], the errors in the ratio $\varepsilon_{81}/\varepsilon_{Comp}$ were about $\pm$ 3%. The errors in the different ratios in eq. (1) were combined in quadrature in order to determine the errors in $d\sigma_{el}/d\Omega$.

The pulse height data obtained at 45° with the 25·2 mg/cm^2 gold target are displayed in figure 3. The 81 keV elastic scattering cross-section in the case of gold at 45° is about

seven times larger than that at backward angles. So at 45°, the 81 keV elastic scattering component is quite visible even in the presence of gold $K\beta'_2$ X-rays of energies between 80·08 and 80·72 keV. The relative transition probabilities for the five main $K\beta'_2$ components turn out to be nearly independent of details of different relativistic theoretical models [8, 9]. So a least-squares-fitting procedure employing the known intensity ratios of the different $K\beta'_2$ components and a common but adjustable pulse height FWHM was used to separate the gold data into seven Gaussians representing contributions from elastic scattering of 81 and 79·6 keV γ rays and gold $K\beta'_2$ X-rays. The fitted individual contributions are indicated by dashed curves. The smooth curve indicating the composite distribution is seen to be in good agreement with experimental data in the energy range of interest above 79·6 keV, the corresponding χ^2 per degree of freedom being 0·7. Note that the fit to experimental data below 79·5 keV is poor on account of the tail of the stronger $K\beta'_1$ X-ray components of lower energy not included in the fitting procedure.

Independent checks of the fitting procedure were also made. For example, a similar analysis of the pulse height data spanning gold $K\alpha_2$ and $K\alpha_1$ X-rays of 66·990 and 68·805 keV, respectively, led to a value of $0{\cdot}585 \pm 0{\cdot}012$ for the intensity ratio of $K\alpha_2$ to $K\alpha_1$ X-rays, which is in agreement with theoretical calculations [8] and previous experiments [10]. Another experiment was performed with 88·03 keV γ rays of a ^{109}Cd source in order to excite only the five gold $K\beta'_2$ X-ray components in the energy range from 79·6 to 81 keV. As expected in this case, only five Gaussians representing the $K\beta'_2$ components were adequate to give excellent fits to the pulse height distributions.

A summary of experimental and theoretical results for cross-sections is presented in table 1. The (MF + ASF) values and S matrix results σ_s obtained with subtraction of spurious resonances are given in columns 2 and 3, respectively. The experimental cross-sections σ_{expt} along with errors $\pm \Delta$ are given in column 4 of table 1. The nature of agreement between σ_{expt} and σ_s is indicated by values of χ_s^2 in column 5, where $\chi_s = (\sigma_{expt} - \sigma_s)/\Delta$. Average values for the different targets of χ_s^2 and of similarly defined $(\chi_{MF+ASF})^2$ are given at the end of the caption of table 1.

4. Results

The experimental results for aluminium ($\varepsilon_K = 1{\cdot}56$ keV) are in good agreement with the different calculated values which differ from each other by less than 2·2%. The values of σ_{expt} for nickel at a few angles show unexpected deviations from the (MF + ASF) or the S matrix calculations. There is good agreement between experiment and S matrix calculations in the case of tantalum and of even gold with a value of ε_K within about 275 eV of the γ energy. The experimental cross-sections for lead ($\varepsilon_K = 88{\cdot}006$ keV) are in fair agreement with S matrix calculations. The (MF + ASF) calculations show significant deviations from experiment in high Z cases at large angles. Except in the case of aluminium, the average values of $(\chi_{MF+ASF})^2$ are larger than unity and are much larger than the corresponding values of χ_s^2, indicating a noticeably poorer agreement of experiment with (MF + ASF) calculations than with calculations based on the S matrix treatment.

Acknowledgement

The work was supported in part by Grant Nos INT-91 02053 and INT-90 19385 of the US National Science Foundation under the Special Foreign Currency programme,

also in part by NSF Grant No. Phy-93 07478, and in part under the auspices of the US Department of Energy by Lawrence Livermore National Laboratory under Contract No. W-7405-ENG-48.

References

[1] G Basavaraju, P P Kane, Lynn D Kissel and R H Pratt, *Phys. Rev.* **A49**, 3664 (1994)
[2] P P Kane, Lynn Kissel, R H Pratt and S C Roy, *Phys. Rep.* **140**, 75 (1986)
[3] The reliability has been tested in a study of elastic scattering of 88·03 keV γ rays by lead for which the value of $(h\nu - \varepsilon_K)$ is only (27 ± 7)eV and the resonant contributions are consequently much larger than the ones in the present study. The test was performed as follows. Extending the S matrix treatment by successive stages to (K), $(K + L)$, $(K + L + M)$ and $(K + L + M + N)$ shells, removing at each stage uncancelled spurious resonances and adding (MF) contributions of remaining electrons, the scattering cross-sections for 125° at $(K + L)$ and $(K + L + M)$ stages were found to differ from the final value at the $(K + L + M + N)$ stage by less than 2·4% and 0·6%, respectively. Further, the cross-section calculated by an S matrix treatment of all occupied shells, requiring an enormously longer computation time but automatically ensuring cancellation of spurious resonances, differed by less than 0·2% from that calculated at the above mentioned $(K + L + M + N)$ stage.
[4] C M Lederer and V S Shirley, *Table of Isotopes*, 7th edn. (Wiley, New York, 1978)
[5] G Basavaraju and P P Kane, in *Proceedings of the eighth symposium on radiation measurements and applications* held at Ann Arbor, Michigan, USA, May 16–19, 1994, *Nucl. Instrum. Methods* **A353**, 209 (1994)
[6] J H Hubbell, Wm J Veigele, E A Briggs, R T Brown, D T Cromer and R J Howerton, *J. Phys. Chem. Ref. Data* **4**, 471 (1975); **6**, 615E (1977)
[7] E Storm and H I Israel, *Nucl. Data Tables* **A7**, 565 (1970)
[8] J H Scofield, *At. Data Nucl. Data Tables* **14**, 121 (1974)
[9] J H Scofield, *Phys. Rev.* **A9**, 1041 (1974)
[10] W Bambynek, B Crasemann, R W Fink, H U Freund, H Mark, C D Swift, R E Price and P V Rao, *Rev. Mod. Phys.* **44**, 716 (1972)